PBC Approach for SMES Devices in Electric Distribution Networks

O. D. Montoya, *Member, IEEE*, W. Gil-González, *Member, IEEE*, and F. M. Serra, *Member, IEEE*

***Abstract*—This express brief presents a nonlinear active and reactive power control for a superconducting magnetic energy storage (SMES) system connected in three-phase distribution networks using pulse-width modulated current-source converter (PWM-CSC). The passivity-based control (PBC) theory is selected as a nonlinear control technique, since the open-loop dynamical model exhibits a port-Hamiltonian (pH) structure. The PBC theory exploits the pH structure of the open-loop dynamical system to design a general control law, which preserves the passive structure in closed-loop via interconnection and damping reassignment. Additionally, the PBC theory guarantees globally asymptotically stability in the sense of Lyapunov for the closed-loop dynamical system. Simulation results in a three-phase radial distribution network show the possibility to control the active and reactive power independently as well as the possibility to use the SMES system connected through a PWM-CSC as a dynamic power factor compensator for time-varying loads. All simulations are conducted in a MATLAB/ODE package.**

***Index Terms*—Superconducting energy storage system (SMES), distribution networks, passivity-based control (PBC), pulse-width modulated current-source converter (PWM-CSC).**

I. Introduction

SUPERCONDUCTING magnetic energy storage (SMES) technology is one of the most promissory energy storage technology, due to its high charge/discharge capability, high energy density and low useful life degradation per cycle of operation, among others [1]. The SMES system is composed by a superconducting coil which is cooled near to absolute zero Kelvin in order to reduce the resistive effect in coil as presented in Fig. 1. The interconnection of the SMES system to the electrical networks requires a power electronic converter [2], [3]. The converter allows to control the total energy stored in the superconducting coil at the same time that permits to control the reactive power interchange between the forced-commutated devices and the AC grid [2]. In this context, there exist possibles power electronic converter technologies that permit to integrate the SMES system to the AC grid. In the first place, it can be used a line-commutated converter (LCC) based on thyristor technology [2]. This technology is not an appropriated option due to that requires active power to feed the thyristor devices, which implies the impossibility to control the reactive power interchange between the converter and the AC grid. Additionally, the LCC produces high harmonic distortion and high active power losses by commutation [2]. In the second place, the SMES system can be integrated by using a voltage source converter (VSC) based on IGBT technology; this converter allows fourth quadrant operation with the active and reactive power control independently [4]. It also produces low harmonic distortion; nevertheless, this interconnection requires a DC/DC converter connected in cascade mode with the VSC in order to control the current in the superconducting coil, which reduces the reliability of the system and the same time that increases the commutation losses [2]. Finally, in third place the SMES system can be integrated using a pulse-width modulated current-source converter (PWM-CSC) based on IGBT technology [2]. The PWM-CSC allows to control the active and reactive power interchange independently with low harmonic distortion. Moreover, it permits to control the superconducting coil current directly, which it does not require additional converters in the DC side increasing the reliability of the whole system [2].

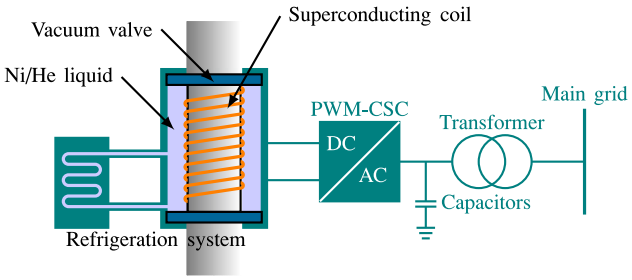

Fig. 1. Typical connection of a SMES system.

Multiple strategies to control SMES systems can be found in the specialized literature, such as linear control by state-feedback [5] and classical proportional-integral controllers [6]–[10], model predictive [11] and fuzzy logic control [12]–[14]. Notwithstanding, the SMES system interconnected with power electronic converter is a nonlinear dynamical system, and there exists few nonlinear control

Manuscript received December 29, 2017; accepted February 9, 2018. Date of publication February 13, 2018; date of current version November 23, 2018. This work was supported in part by the National Scholarship Program Doctorates of the Administrative Department of Science, Technology and Innovation of Colombia under Grant 727-2015, in part by Ph.D. Program in Engineering of Universidad Tecnológica de Pereira, Colombia, and in part by Universidad Nacional de San Luis, Argentina, and Consejo Nacional de Investigaciones Cientficas y Técnicas, Argentina. This brief was recommended by Associate Editor T. Fernando. *(Corresponding author: O. D. Montoya.)*

O. D. Montoya is with the Programa de Ingeniería Eléctrica y Electrónica, Universidad Tecnológica de Bolívar, Cartagena 131001, Colombia (e-mail: o.d.montoyagiraldo@ieee.org).

W. Gil-González is with the Programa de Ingeniería Eléctrica, Universidad Tecnológica de Pereira, Pereira 660003, Colombia (e-mail: wjgil@utp.edu.co).

F. M. Serra is with the Laboratorio de Control Automático, Universidad Nacional de San Luis, San Luis 5700, Argentina (e-mail: fserra@ieee.org).

Color versions of one or more of the figures in this paper are available online at http://ieeexplore.ieee.org.

Digital Object Identifier 10.1109/TCSII.2018.2805774

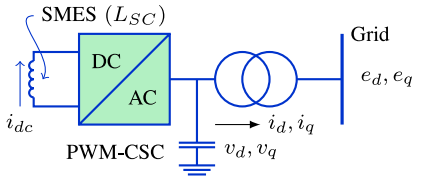

Fig. 2. Circuital connection between a SMES system and the three-phase electrical network.

strategies applied on it [15], [16]. Further, none of these controllers guarantee global stability conditions in closed-loop which is proposed in this brief. To the best knowledge of the authors', there exists only one passivity-based control (PBC) approximation to operate a three-phase SMES system in microgrids [17]. Nevertheless, the control presented in that work does not allow to control the active and reactive power independently as is proposed here.

The main contribution of this brief is the possibility to control the active and reactive power independently in a SMES systems connected through PWM-CSC to the AC grid for distribution applications. A PBC theory is selected as control technique since it allows a nonlinear controller design that guarantees global asymptotic stability conditions in closed-loop.

II. Dynamical Model

The electrical connection for the SMES system presented in Fig. 2 can be modeled as five ordinary nonlinear differential equations by applying Kirchhoff's laws in the AC side of the converter and the Tellegen's theorem in both sides of the converter [17]. These differential equations are presented as follows using the *dq* reference frame via Park's transformation. Notice that the superconducting coil resistance is not considered because the refrigeration system reduces this effect near to zero values.

$$\begin{aligned} L_T\frac{d}{dt}i_d &= -R_T i_d - \omega L_T i_q + v_d - e_d,\\ L_T\frac{d}{dt}i_q &= -R_T i_q + \omega L_T i_d + v_q - e_q,\\ C\frac{d}{dt}v_d &= -i_d - \omega C v_q + m_d i_{dc},\\ C\frac{d}{dt}v_q &= -i_q + \omega C v_d + m_q i_{dc},\\ L_{SC}\frac{d}{dt}i_{dc} &= -m_d v_d - m_q v_q, \end{aligned} \tag{1}$$

where e_d and e_q are the direct and quadrature voltages values of the AC equivalent node, L_T and R_T are the inductance and resistive parameters of the transformer, ω is the electrical frequency of the AC equivalent node, i_d and i_q are the direct and quadrature current signals through of the transformer, L_{SC} corresponds to the inductance value of the superconducting coil device and i_{dc} is the DC current flowing between their terminals. Finally, m_d and m_q are the direct and quadrature modulation indexes which correspond to the control signals.

The dynamical model defined by (1) can be represented as a port-Hamiltonian (pH) system defining the following state variables: $x_1 = L_T i_d$, $x_2 = L_T i_q$, $x_3 = C v_d$, $x_4 = C v_q$ and $x_5 = L_{SC} i_{dc}$ as shows:

$$\dot{x} = [\mathcal{J}(u) - \mathcal{R}]\nabla\mathcal{H}(x) + \mathcal{E}, \tag{2}$$

where x are the state variables, u corresponds to the control signals (m_d and m_q), $\mathcal{J}(u)$ represents the interconnection matrix, $\mathcal{R}$ is the dissipation matrix, $\mathcal{E}$ are the external inputs and $\mathcal{H}(x)$ corresponds to the Hamilton function known as energy storage function of the system. With the aforementioned conditions, it is important to mention that the dynamical system given by (2) is a passive dynamical system [18], [19].

All terms in (2) can be easily obtained by comparison with (1). These terms are defined as follows:

$$\begin{aligned} \mathcal{J}(u) - \mathcal{R} &= \begin{bmatrix} -R_T & -\omega L_T & 1 & 0 & 0\\ \omega L_T & -R_T & 0 & 1 & 0\\ -1 & 0 & 0 & -\omega C & m_d\\ 0 & -1 & \omega C & 0 & m_q\\ 0 & 0 & -m_d & -m_q & 0 \end{bmatrix},\\ \mathcal{H}(x) &= \frac{1}{2L_T}\left(x_1^2 + x_2^2\right) + \frac{1}{2C}\left(x_3^2 + x_4^2\right) + \frac{1}{2L_{SC}}x_5^2,\\ \mathcal{E} &= -\begin{bmatrix} e_d & e_q & 0 & 0 & 0 \end{bmatrix}^T. \end{aligned} \tag{3}$$

Notice that $\nabla\mathcal{H}(x)$ in (2) corresponds to the gradient operator applied over the Hamiltonian function $\mathcal{H}(x)$.

III. Passivity-Based Control Framework

The PBC allows to obtain a general control law that can be applied on linear/nonlinear autonomous/non-autonomous dynamical systems, modeled as Hamiltonian systems, known in specialized literature as pH systems [20]–[22]. The main idea of a PBC design is to transform an open-loop dynamical system in a closed-loop dynamical system via modification of the dynamic structure of the system [23], [24].

In general way a closed-loop formulation uses the Hamiltonian function and interconnection and damping matrices to obtain the desired dynamical behavior of the state variables [17]. This calculation is presented as follows:

$$\dot{x}(t) = [\mathcal{J}_\mathcal{D} - \mathcal{R}_\mathcal{D}]\nabla\mathcal{H}_\mathcal{D}(x), \tag{4}$$

where $\mathcal{J}_\mathcal{D}$ and $\mathcal{R}_\mathcal{D}$ correspond to the desired interconnection and damping matrices, $\mathcal{H}_\mathcal{D}(x)$ is the desired Hamilton function and x is the desired dynamic closed-loop. Additionally, $\mathcal{J}_\mathcal{D}$ is antisymmetric defined ($\mathcal{J}_\mathcal{D} = -\mathcal{J}_\mathcal{D}^T$) and $\mathcal{R}_\mathcal{D}$ is a positive-definite matrix ($\mathcal{R}_\mathcal{D} \succ 0$). Taking into account these definitions the desired dynamical systems is globally asymptotically stable in the sense of Lyapunov [25].

The design of a controller using Interconnection Damping Assignment-Passivity-Based Control (IDA-PBC) formulation has three degrees of freedom to determine $\mathcal{J}_\mathcal{D}$, $\mathcal{R}_\mathcal{D}$ and $\mathcal{H}_\mathcal{D}$ [21], [26].

The general control law for the dynamical system is obtained by comparison between open-loop and closed-loop formulations shown in (2) and (4), which produces:

$$[\mathcal{J}_\mathcal{D} - \mathcal{R}_\mathcal{D}]\nabla\mathcal{H}_\mathcal{D}(x) = [\mathcal{J}(u) - \mathcal{R}]\nabla\mathcal{H}(x) + \mathcal{E}. \tag{5}$$

The control input can be obtained solving the set of equations from (5) [25].

IV. Control Design

The PBC technique is employed to design the controller for the SMES system with PWM-CSC. We select this strategy, since the open-loop dynamical system has a natural pH representation which simplifies the control design in closed-loop; additionally, it is possible to guarantee global asymptotically stable operation under this design [21].

Considering the open-loop Hamilton system presented by (2) and (3). We select the following desired interconnection and damping matrices, and the Hamilton desired energy storage function preserving the structure presented in (3) in closed-loop, as follows:

$$\mathcal{J}_{\mathcal{D}} - \mathcal{R}_{\mathcal{D}} = -\begin{bmatrix} R_1 & 0 & k_{13} & 0 & 0 \\ 0 & R_2 & 0 & k_{24} & 0 \\ -k_{13} & 0 & R_3 & 0 & 0 \\ 0 & -k_{24} & 0 & R_4 & 0 \\ 0 & 0 & 0 & 0 & R_5 \end{bmatrix},$$

$$\mathcal{H}_{\mathcal{D}}(x) = \begin{pmatrix} \frac{1}{2L_T}\left(\left(x_1 - x_1^r\right)^2 + \left(x_2 - x_2^r\right)^2\right) \\ + \frac{1}{2C}\left(\left(x_3 - x_3^r\right)^2 + \left(x_4 - x_4^r\right)^2\right) \\ + \frac{1}{2L_{SC}}\left(x_5 - x_5^r\right)^2 \end{pmatrix}. \quad (6)$$

Notice that $R_i > 0$ $i = 1, 2, \ldots, 5$, and x_i^r, $i = 1, 2, \ldots, 5$ are the reference values of the state variables defined as follows: $x_1^r = L_T i_d^r$, $x_2^r = L_T i_q^r$, $x_3^r = C v_d^r$, $x_4^r = C v_q^r$ and $x_5^r = L_{SC} i_{dc}^r$; additionally, $\{k_{13}, k_{24}\} \in \mathbb{R}$.

The desired Hamiltonian function $\mathcal{H}_{\mathcal{D}}(x)$ has a global minimum in x_i^r, $i = 1, 2, \ldots, 5$, which implies that the closed-loop dynamical system is globally asymptotically stable at this desired point of operation.

To obtain a general control law are solved the third and fourth rows in (5) which produce:

$$m_d = \frac{1}{i_{dc}}\left(i_d - R_3\left(v_d - v_d^r\right) + k_{13}\left(i_d - i_d^r\right) - C\omega v_q\right),$$
$$m_q = \frac{1}{i_{dc}}\left(i_q - R_4\left(v_q - v_q^r\right) + k_{24}\left(i_q - i_q^r\right) + C\omega v_d\right). \quad (7)$$

The control laws (7) are algebraic equations and integral calculations are not required in their implementation. This shows that the proposed control has low computational complexity.

To control the active and reactive power independently, it is necessary to find the relation between the active and reactive power with the AC grid voltage and the AC current through the three-phase transformer. This relationship is presented below [17]:

$$i_d^r = \left(\frac{1}{e_d^2 + e_q^2}\right)\left(e_d p_{ac}^r \alpha + e_q q_{ac}^r\right),$$
$$i_q^r = \left(\frac{1}{e_d^2 + e_q^2}\right)\left(e_q p_{ac}^r \alpha - e_d q_{ac}^r\right), \quad (8)$$

where p_{ac}^r and q_{ac}^r are the desired active and reactive power outputs, and α guarantees that the superconducting coil never overpass its maximum and minimum capabilities. α can be calculated as:

$$\alpha = \begin{cases} 1 & i_{dc}^{\min} \le i_{dc} \le i_{dc}^{\max}, \\ 0 & \text{otherwise.} \end{cases} \quad (9)$$

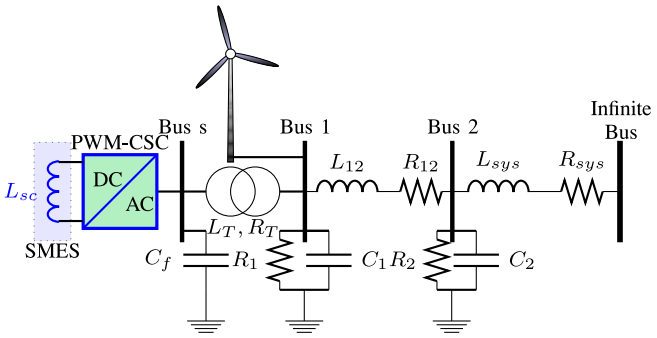

Fig. 3. Distribution network.

TABLE I
Parameters for Simulation

Parameter	Value	Unit	Parameter	Value	Unit
L_{sys}	2.5	mH	R_{sys}	5	$m\Omega$
L_{12}	1.5	mH	R_{12}	10	$m\Omega$
L_T	2.5	mH	R_T	1.25	$m\Omega$
L_{SC}	7.5	H	R_1	1	Ω
R_2	1	Ω	C_1	0.1	μF
C_2	0.1	μF	C_f	160	μF
i_{dc}^{min}	25	A	i_{dc}^{max}	100	A
v_{LL}^{rms}	440	V	-	-	-

In order to control i_d and i_q currents, from (5) are solving the reference values for v_d and v_q using its first two equations as follows:

$$v_d^r = -\frac{1}{k_{13}}\begin{pmatrix} e_d - v_d - R_1\left(i_d - i_d^r\right) \\ + R_T i_d - k_{13} v_d + L_T \omega i_q \end{pmatrix},$$
$$v_q^r = \frac{1}{k_{24}}\begin{pmatrix} v_q - e_q + R_2\left(i_q - i_q^r\right) \\ - R_T i_q + k_{24} v_q + L_T \omega i_d \end{pmatrix}. \quad (10)$$

Notice that k_{13} and k_{24} cannot take zero values. Finally, to know the dynamical behavior of i_{dc} current, from the last equation of (5) it is obtained its reference value as shows:

$$i_{dc}^r = \frac{1}{R_5}\left(R_5 i_{dc} - m_d v_d - m_q v_q\right). \quad (11)$$

V. Test System and Simulation Results

A. The Studied System

Fig. 3 illustrates the test system which has a SMES system connected in bus-1 through of a PWM-CSC (see Fig. 2). Additionally, all parameters of the electrical grid are shown in Table I.

To evaluate the capability, robustness and effectiveness of the proposed controller it is comparing with a conventional PI controller. The simulations are carry-out in MATLAB software using ordinary differential equation packages ODE15s/ODE23tb. In addition, the parameters of the conventional PI controller and the proposed controller are adjusted in such a way to obtain an equal dynamic response, in order to be able to comparisons fair. All data of the PBC and the conventional PI controller are shown in Tables II and III, respectively.

B. Active and Reactive Power Control

In this part, it is demonstrated the capacity of the proposed strategy to control the active and reactive power (p_{ac} and q_{ac})

TABLE II
PBC PARAMETERS

k_{13}	k_{24}	R_1	R_2	R_3	R_4	R_5
-10	-10	100	100	1000	1000	100

TABLE III
PI CONTROLLER PARAMETERS

v_d^{ref}		v_q^{ref}		i_d^{ref}		m_q^{ref}	
K_p	K_i	K_p	K_i	K_p	K_i	K_p	K_i
15	5	15	5	200	300	200	300

TABLE IV
ACTIVE AND REACTIVE POWER REFERENCES

p_{ac}^{ref} [kW]	t_i [s]	t_f [s]	q_{ac}^{ref} [kVAr]	t_i [s]	t_f [s]
0	0	0.1	0	0	0.3
4.5	0.1	0.5	−5	0.3	0.7
−4	0.5	0.9	3.5	0.7	0.9
3	0.9	1.0	−2	0.9	1.0

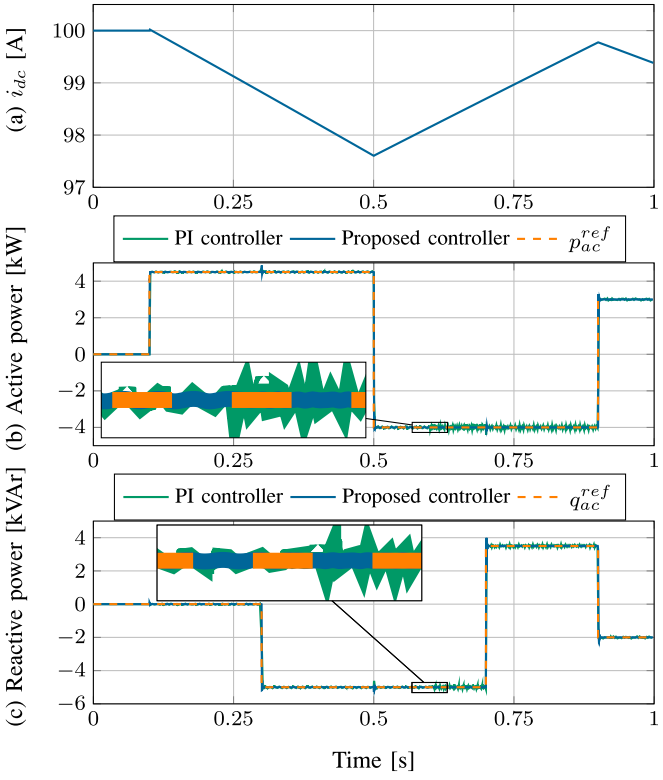

Fig. 4. Dynamical response of active and reactive power control of the SMES system: (a) superconducting coil current i_{dc}, (b) active power delivered by SMES system p_{ac} and (c) reactive power delivered by SMES system q_{ac}.

on the bus-1. The reference values for active and reactive power are chosen in such a way that have the possibility to control active and reactive power in independent and bidirectional form, as is shown in Table IV.

It is also considered that in the infinite bus there exists a 10% of unbalance in each phase as follows: $|e_a(t)| = 1.0v_{LL}^{rms}$, $|v_b(t)| = 0.9v_{LL}^{rms}$ and $|v_c(t)| = 1.1v_{LL}^{rms}$, respectively; this consideration is from 0 s to 0.6 s. The time simulation from 0.6 s to 1 s, it is considered a high harmonic distortion in the infinite bus, as shown in (12) for the a-phase. The other phases

TABLE V
INDUCTION GENERATOR PARAMETERS

v_{LL}^{rms}	$r_1[\Omega]$	$r_2[\Omega]$	$X_1[\Omega]$	$X_2[\Omega]$	$X_m[\Omega]$
440	0.641	0.332	1.106	0.464	78.9

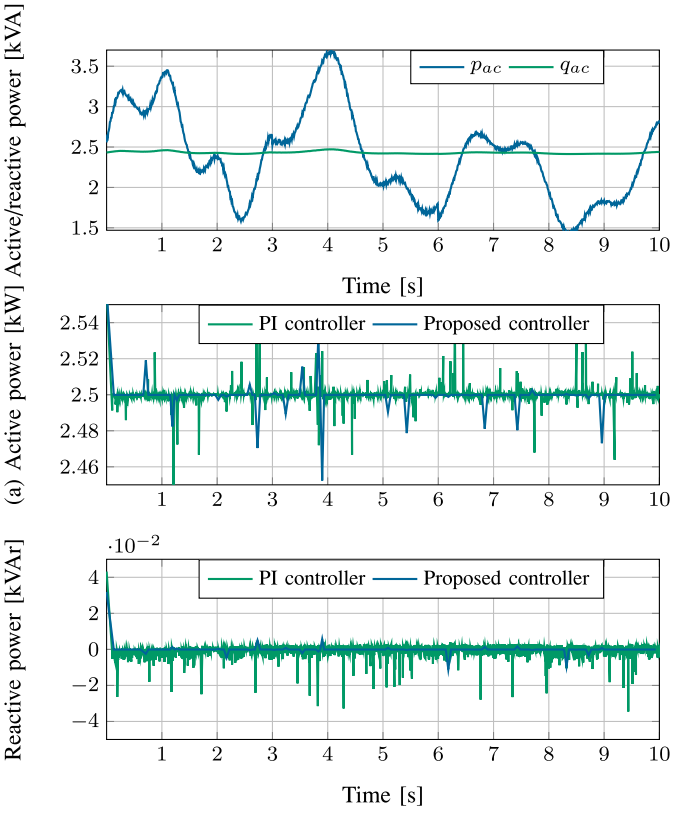

Fig. 5. Dynamical response of the active and reactive power control in SMES system to compensate oscillations caused by variations in the speed of wind in the wind generator.

are defined similarly that a-phase using positive sequence. Additionally, it is assumed that the SMES system has been charged until its maximum current value (see Table I).

$$v_a(t) = \sqrt{\frac{2}{3}}440\begin{bmatrix} \cos(\omega t)+ \\ \frac{2}{5}\cos\left(5\omega t - \frac{\pi}{6}\right)+ \\ \frac{1}{5}\cos\left(7\omega t - \frac{\pi}{3}\right) \end{bmatrix} V. \tag{12}$$

Fig. 4a depicts the dynamical behavior at the DC side of the SMES system when this is used to control active and reactive power (see Figs. 4b and 4c respectively).

Comparing Figs. 4a and 4b can be observed that the i_{dc} current is directly influenced by the behavior of the active power. This allows to control the energy stored indirectly with the active power control.

Figs. 4b and 4c show the performance of the proposed control and the conventional PI to control the active and reactive of the SMES system. Both controls respond adequately; however, the proposed control has a better performance, since presents smaller oscillations. Additionally, it can also be observed that the power oscillations increase considerably when harmonic distortion appears.

C. Support Active and Reactive Power

In this part, it is shown the possibility of the SMES systems to support active and reactive power for distributed generation applications connecting a wind turbine generator type-A connected in the bus-1 (see Fig. 3). This wind turbine generator injects active power and absorbs reactive power from the AC grid. The induction generator parameters given in Table V were taking from [27].

It is considered that the wind generator has been dispatched with an active power generation of $2.5kW$. However, the active power supplied is not constant and this depends of the wind speed variations; which can generate economic penalizations. Fig. 5a shows the active power generated of the wind turbine and as well as its reactive power consumption.

The objective is to support the active power oscillations using a SMES system and to compensate all reactive power required by the induction generator. Figs. 5b and 5c show the active and reactive power output in the bus-1.

Figs. 5b and 5c show the accuracy of the proposed control to support the active and reactive power in the electric distribution systems with DERs. In this part, the active power has a standard deviation of 0.8 % and 1.1 % for the proposed control and conventional PI controller respectively. Also, the reactive power is kept at 0 $kVAr$ and thus improving the power factor in bus-1.

VI. Conclusion and Future Work

In this brief an IDA-PBC strategy to operate the SMES system connected to an electric distribution network through a PWM-CSC was presented. The proposed control methodology using passivity theory guarantees global asymptotic stability of the dynamical system in the sense of Lyapunov. The proposed control scheme showed a good performance to control of active and reactive power in the SMES system for all cases proposed which considering unbalance and high harmonic distortion in the voltage provide by the AC grid. It is also considered the possibility to support of active power oscillations and the reactive power in the electric distribution systems with DERs. It is worth noting that the proposed control always had a better response than conventional PI controller in all cases analyzed in this brief, which makes it an attractive control strategy to be applied in the support the active and reactive power in distribution networks.

As future work can be proposed a full dynamical model that considers all elements presents in radial distribution networks, in order to design a general control strategy to operate whole grid passivity-based control theory, taking advantage of the passivity nature structure of the electrical networks. Additionally, can be used the proposed control strategy for SMES system enhance stability operation in power systems.

References

[1] B. Zakeri and S. Syri, "Electrical energy storage systems: A comparative life cycle cost analysis," *Renew. Sustain. Energy Rev.*, vol. 42, pp. 569–596, Feb. 2015.

[2] M. H. Ali, B. Wu, and R. A. Dougal, "An overview of SMES applications in power and energy systems," *IEEE Trans. Sustain. Energy*, vol. 1, no. 1, pp. 38–47, Apr. 2010.

[3] A. Zobaa, Ed., *Energy Storage—Technologies and Applications*. Rijeka, Croatia: InTech, 2013.

[4] J. Shi *et al.*, "SMES based dynamic voltage restorer for voltage fluctuations compensation," *IEEE Trans. Appl. Supercond.*, vol. 20, no. 3, pp. 1360–1364, Jun. 2010.

[5] W. Gil-González, O. D. Montoya, A. Garcés, and A. Escobar-Mejía, "Supervisory LMI-based state-feedback control for current source power conditioning of SMES," in *Proc. 9th Annu. IEEE Green Technol. Conf. (GreenTech)*, Denver, CO, USA, Mar. 2017, pp. 145–150.

[6] A. Ortega and F. Milano, "Generalized model of VSC-based energy storage systems for transient stability analysis," *IEEE Trans. Power Syst.*, vol. 31, no. 5, pp. 3369–3380, Sep. 2016.

[7] H. Hayashi *et al.*, "Test results of power system control by experimental SMES," *IEEE Trans. Appl. Supercond.*, vol. 16, no. 2, pp. 598–601, Jun. 2006.

[8] J. Shi, Y. Tang, L. Ren, J. Li, and S. Cheng, "Discretization-based decoupled state-feedback control for current source power conditioning system of SMES," *IEEE Trans. Power Del.*, vol. 23, no. 4, pp. 2097–2104, Oct. 2008.

[9] I. Ngamroo, "Simultaneous optimization of SMES coil size and control parameters for robust power system stabilization," *IEEE Trans. Appl. Supercond.*, vol. 21, no. 3, pp. 1358–1361, Jun. 2011.

[10] Z. Wang, Z. Zou, and Y. Zheng, "Design and control of a photovoltaic energy and SMES hybrid system with current-source grid inverter," *IEEE Trans. Appl. Supercond.*, vol. 23, no. 3, p. 5701505, Jun. 2013.

[11] T.-T. Nguyen, H.-J. Yoo, and H.-M. Kim, "Applying model predictive control to SMES system in microgrids for eddy current losses reduction," *IEEE Trans. Appl. Supercond.*, vol. 26, no. 4, pp. 1–5, Jun. 2016.

[12] S. Wang and J. Jin, "Design and analysis of a fuzzy logic controlled SMES system," *IEEE Trans. Appl. Supercond.*, vol. 24, no. 5, pp. 1–5, Oct. 2014.

[13] A. M. Hemeida, "A fuzzy logic controlled superconducting magnetic energy storage, SMES frequency stabilizer," *Elect. Power Syst. Res.*, vol. 80, no. 6, pp. 651–656, Jun. 2010.

[14] M. H. Ali, B. Wu, J. Tamura, and R. A. Dougal, "Minimization of shaft oscillations by fuzzy controlled SMES considering time delay," *Elect. Power Syst. Res.*, vol. 80, no. 7, pp. 770–777, Jul. 2010.

[15] F. Liu *et al.*, "Experimental evaluation of nonlinear robust control for SMES to improve the transient stability of power systems," *IEEE Trans. Energy Convers.*, vol. 19, no. 4, pp. 774–782, Dec. 2004.

[16] M. A. Mahmud, M. J. Hossain, and H. R. Pota, "Dynamical modeling and nonlinear control of superconducting magnetic energy systems: Applications in power systems," in *Proc. Aust. Universities Power Eng. Conf. (AUPEC)*, Perth, WA, Australia, Sep./Oct. 2014, pp. 1–6.

[17] W. Gil-González, O. D. Montoya, A. Garcés, and G. Espinosa-Pérez, "IDA-passivity-based control for superconducting magnetic energy storage with PWM-CSC," in *Proc. 9th Annu. IEEE Green Technol. Conf. (GreenTech)*, Denver, CO, USA, Mar. 2017, pp. 89–95.

[18] Y. Gao, B. Sun, and G. Lu, "Passivity-based integral sliding-mode control of uncertain singularly perturbed systems," *IEEE Trans. Circuits Syst. II, Exp. Briefs*, vol. 58, no. 6, pp. 386–390, Jun. 2011.

[19] Y. Gao, G. Lu, and Z. Wang, "Passivity analysis of uncertain singularly perturbed systems," *IEEE Trans. Circuits Syst. II, Exp. Briefs*, vol. 57, no. 6, pp. 486–490, Jun. 2010.

[20] S. Sanchez, R. Ortega, R. Griño, G. Bergna, and M. Molinas, "Conditions for existence of equilibria of systems with constant power loads," *IEEE Trans. Circuits Syst. I, Reg. Papers*, vol. 61, no. 7, pp. 2204–2211, Jul. 2014.

[21] S. P. Nageshrao, G. A. D. Lopes, D. Jeltsema, and R. Babuska, "Port-Hamiltonian systems in adaptive and learning control: A survey," *IEEE Trans. Autom. Control*, vol. 61, no. 5, pp. 1223–1238, May 2016.

[22] J. Li, Y. Liu, C. Li, and B. Chu, "Passivity-based nonlinear excitation control of power systems with structure matrix reassignment," *Information*, vol. 4, no. 3, pp. 342–350, Aug. 2013.

[23] R. Ortega, J. Perez, P. Nicklasson, and H. Sira-Ramirez, *Passivity-Based Control of Euler–Lagrange Systems: Mechanical, Electrical and Electromechanical Applications*, 1st ed. London, U.K.: Springer, 1998.

[24] R. Ortega, A. van der Schaft, B. Maschke, and G. Escobar, "Interconnection and damping assignment passivity-based control of port-controlled Hamiltonian systems," *Automatica*, vol. 38, no. 4, pp. 585–596, Apr. 2002.

[25] F. M. Serra and C. H. D. Angelo, "IDA-PBC controller design for grid connected front end converters under non-ideal grid conditions," *Elect. Power Syst. Res.*, vol. 142, pp. 12–19, Jan. 2017.

[26] C. Gaviria, E. Fossas, and R. Grino, "Robust controller for a full-bridge rectifier using the IDA approach and GSSA modeling," *IEEE Trans. Circuits Syst. I, Reg. Papers*, vol. 52, no. 3, pp. 609–616, Mar. 2005.

[27] S. Chapman, *Electric Machinery Fundamentals*, 5th ed. New York, NY, USA: McGraw-Hill, 2005.